Development of a Co-20Cr alloy for potential biomedical applications

Ana Ramirez-Ledesma[1], Hugo Lopez F[2*], Julio Juarez-Islas[1]

[1]Instituto de Investigaciones en Materiales, Universidad Nacional Autonoma de Mexico, Av. Universidad 3000, Circuito Exterior S/N, Cd. Universitaria, 04510, Mexico, D. F., Mexico,
[2]Materials Science and Engineering Department, CEAS, University of Wisconsin-Milwaukee 3200 N. Cramer Street, Milwaukee WI 53211, USA

[*]Corresponding author

DOI: 10.5185/amlett.2018.1586
www.vbripress.com/aml

Abstract

A Co-20 wt. Cr alloy was vacuum induction melted and cast into a wedge shaped copper mold. The resultant microstructures were investigated from sections obtained longitudinally and centrally in the plane normal to the diverging wedge faces. The aim of this work was to produce a microstructure free of interdendritic segregation with minimal or no intermetallic precipitates and suitable for biomedical implant applications. The as-cast microstructure consisted predominantly of columnar dendrites. In particular, the presence of athermal HCP ε-martensite and the metastable FCC γ-Co phase were identified by X-ray diffraction means and scanning electron microscopy. It was found that the exhibited volume fraction of athermal ε-martensite was over 90 wt. %. In addition, a heat treating below the γ/ε transition temperature led to transformation of the athermal ε-martensite into a stress-relieved isothermal one. In turn, the resultant tensile properties, ductility and fracture mode of the alloy after the heat treatment exhibited significant changes. Finally, preliminary tests in artificial saliva indicated that the heat-treated alloy possesses appreciable corrosion resistance when compared with other Co-alloys, making it an ideal candidate for dental implants. Copyright © 2018 VBRI Press.

Keywords: Cobalt alloys, rapid solidification, athermal martensite, biomedical alloys.

Introduction

There are currently, considerable efforts into the development of new versions of biomedical grade cobalt alloys with unique tribological properties and a combination of suitable mechanical properties, including fatigue strength [**1-3**] and alloy biocompatibility [**4,5**]. Conventional Co-Cr-Mo-C alloys (ASTM F75) solidified using investment casting techniques account for most of the available HIP and knee implants. Nevertheless, there have been numerous developments aimed at improving the microstructural design of these alloys in order to achieve improved properties including biocompatibility. Among these efforts, low carbon as-cast Co-alloys, powder metallurgy processed and wrought BioDur CCM alloy versions with improved wear resistance have been produced [**6**]**.**

Alternatively, carbon additions have been replaced by nitrogen and novel versions of cobalt alloys have been designed **[7]**. In addition, alloy thermal mechanical processing and grain size control have been implemented to improve alloy strength **[8]**. Other efforts have been related to alloy heat treatments aimed at the development of fully isothermal ε (HCP) martensite from the high temperature γ (FCC) phase [**9**]. It is well known that the ε-phase possess improved wear properties when compared with γ (FCC) matrix-phase [**10**]. However, the alloy strength and biocompatibility might not be optimal when compared with predominantly FCC γ-matrix alloys.

More recently [**11**], a novel approach based on rapid solidification processing has been reported for the development of Co-alloys with unique properties for biomedical applications.

From the extensive works reported on ASTM-F75 Co-based alloys, it is clearly evident that the thermodynamically stable phase at room temperature should be the ε-phase. Nevertheless, upon cooling from the high temperature γ (FCC) phase, the athermal HCP ε-martensite transformation is rather sluggish and it never goes to completion [**12**]. The exhibited amounts of athermal martensite in as-cast Co-alloys are typically of the order of 10-20 wt. pct. Among the main factors that hinder the athermal γ to ε martensitic transformation are (a) the annealing temperatures employed [**12**], (b) grain size effects [**13**]and (c) alloy cooling rates [**11**].

From the work of Saldivar et al [**12**], it is evident that increasing the solid solution temperatures (between 1040-1250^{o}C) within the γ-phase field coupled with increasing annealing times (i. e from 1 minute to 1 hour) promotes an increase in the amount of athermal

ε-martensite upon quenching in a Co-27Cr-5Mo-0.05C alloy. In turn, this suggests that the development of ε-nucleation sites for the transformation to athermal ε-martensite is favored by high temperature anneals and by increasing the annealing exposure times. Nevertheless, the maximum volume fraction of transformed athermal ε-martensite only reaches a maximum of up to 20 wt. % in most cases.

These observations are in agreement with the suggestions of Olsen and Cohen [**14**] related to the critical configuration of ε-martensite embryos. In his work, he considers that the density of potential ε-martensite embryos is rather sluggish (of the order of 10^6 embryos/cm^3) to provide a full γ to ε transformation. Moreover, from the work of P. Huang et al [**13**], it has been found that a reduction in grain size inhibits the formation of athermal ε-martensite. In their work they found that the amount of athermal ε-martensite obtained when the alloy grain size was 10 μm conditions was around 12 vol. % but it increased up to 70 % when the grain size was increased to 324 μm through heat treating.

Other factors such as alloy content are also expected to contribute to the extent of the transformation as they effect the alloy stacking fault energy (γ_{SF}). Nevertheless, there are limited reports on any specific roles. As for the effect of interstitials such as C and N, it is apparent that their solubility in the ε-martensite phase is negligible [**9**]. In recent works [**15**], it has been found that rapid solidification from the liquid state in Co alloys such as in tungsten inert gas (TIG) surface modification, the exhibited amounts of athermal ε-martensite can reach up to 70 wt. %. In this case rapid solidification occurs in the melt pool induced by TIG. In turn, it is likely that the defect configurations for ε-martensite embryo formation are strongly favored by rapid alloy cooling effects. Further work on rapid solidification effects on the exhibited amount of athermal ε-martensite have been investigated [**16**]. From this work, it is found that at very high solidification rates such as those imposed by laser melting a transition from a dendritic solidification front to a cellular one occurs which is accompanied by a total absence of the ε–martensite phase.

In this work, a Co-20Cr alloy was melted by employing a high vacuum furnace and a water cooled V-shaped mold to induce rapid solidification. The as-cast alloy, was microstructurally characterized and properties such as strength end elongation were determined, including alloy biocompatibility.

Experimental

In this work a binary Co-20Cr alloy was produced by vacuum induction melting. The alloy was melted and then cast into water cooled wedge V-copper shaped molds (see **Fig. 1**) in order to induce rapid solidification at various solidification rates.

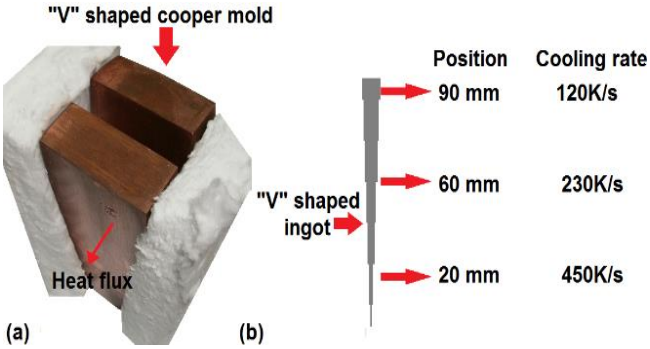

Fig. 1. (a) Wedge shaped copper mold isolated in both sides by an alumina sheet, (b) "V" shaped ingot showing three different cooling rate zones: 90 mm high-120 K/s, 60 mm high-230 K/s and 20 mm high-450 K/s.

Notice that depending on the wedge thickness location, cooling rates vary from 120 K/s to 450 K/s. Moreover, flat copper molds were used to cast flat bars at a constant cooling rate within the rapid solidification regime. V-shaped Cu mold and corresponding cooling rates along the wedge shaped casting.

The flat cast-samples were employed for determinations of mechanical properties and corrosion behavior. Under a constant rapid solidification rate. This was followed by metallographic preparation of samples for optical, scanning electron microscopy (SEM) and transmission electron microscopy (TEM). The amounts of athermal ε-martensite were determined from X-ray diffraction results and by using the expression proposed by Sage and Guillaud [**17**].

$$HCP\ (wt.\%) = \frac{I(10\bar{1}1)_{HCP}}{I(10\bar{1}1)_{HCP}+1.5\,I(200)_{FCC}} \quad (1)$$

The alloy biocompatibility was determined by corrosion testing from potentiodynamic polarization curves obtained in a Gill AC potentiostat and by employing a solution that resembles saliva (see **Table 1**).

Table 1. Chemical composition of the artificial saliva.

Compound	Quantity (g/l)
KH_2PO_4	0.34
$Na_2HPO_4.2H_2O$	0.445
$KHCO_3$	1.5
NaCl	0.585
$MgCl_2.6H_2O$	0.0305
Citric acid	0.0315
$CaCl_2$	0.0166

Finally, the alloy tensile properties were measured from tensile testing bars machined from rapidly solidified flat castings.

Results and discussion

Development of athermal e-martensite

In general, the exhibited microstructure was predominantly dendritic, with dendrite sizes decreasing at increasing solidification rates. Nevertheless near the tip of the wedge shaped castings, the cast microstructure became equiaxial. **Fig. 2** shows the exhibited dendritic solidification structure.

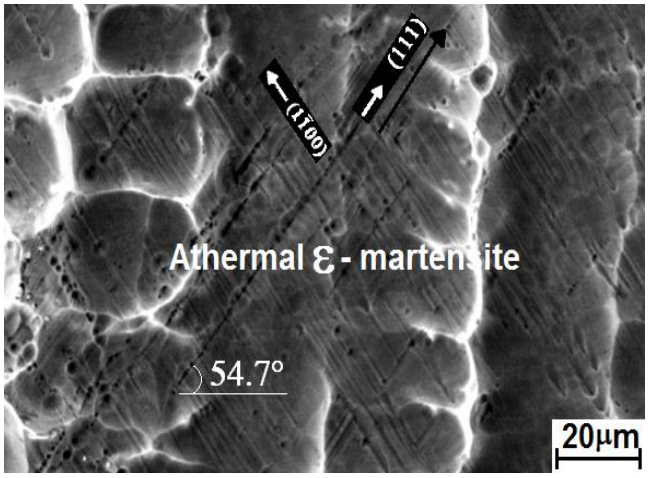

Fig. 2. As-cast Co-20 wt. %Cr microstructure: SEM micrograph of the FCC γ-Co dendrites and athermal ε-martensite formed inside the dendrites.

In particular, notice the relatively elevated amounts of athermal ε-martensite (see numerous striations within dendrites associated with the athermal martensite). **Fig. 3** shows the X-ray diffraction peaks exhibited by the rapidly solidified alloy with a thickness section of 90 mm.

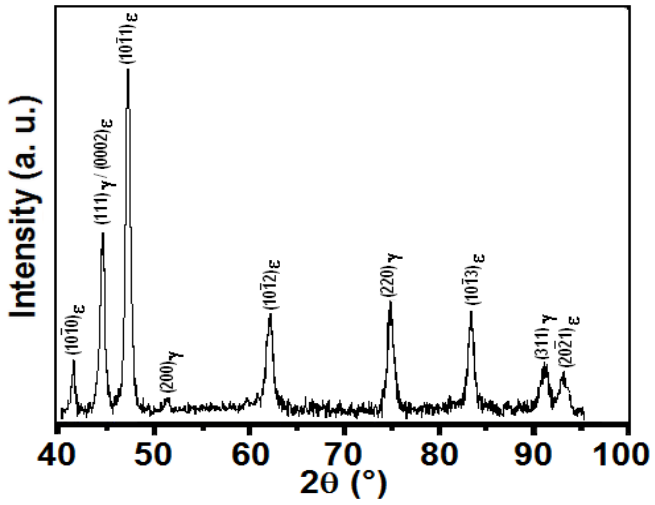

Fig. 3. X-ray intensity peaks showing the presence of ε-martensite and the γ-phase.

Using the expression of Sage and Guillaud [**17**] the estimated volume fractions of athermal ε-martensite were 92.6 vol. %. Apparently rapid solidification promotes the development of athermal ε-martensite which can be as high as over 90 %. However, when the dendritic grain structure becomes equiaxial, the exhibited amounts of athermal ε-martensite significantly decrease (i e down to almost none). Apparently, long columnar dendritic grains strongly favor the development of athermal ε-martensite.

Fig. 4 are TEM micrographs showing a large density of stacking faults and of ε-martensite present in the Co-20Cr alloy after rapid solidification. Notice that in between ε-martensite plates, residual γ-phase can be present. In addition, there is a relatively large density of stacking faults and ε -martensite as expected when the conditions for ε-nucleation are highly favored **[14]**.

From the work of Olson and Cohen [**14**] it is found that when the alloy stacking fault energy (γ_{SF}) becomes zero or negative, ε-martensite embryos can be formed spontaneously. The nucleation defect being a faulting mechanism consisting of a group of lattice dislocations where the motion of a Shockley partial on every second FCC closed packed plane gives rise to an ε-phase nucleus. Among the possible faulting defects suggested are intrinsic stacking faults, twin intersections, incoherent twins or inclusion interfaces [**14**]. From this work it is apparent that when the undercooling associated with the γ to ε transformation is suddenly too large such as in rapid solidification, the defects necessary for the development of critically sized embryos are drastically increased leading to almost 100 vol. % athermal ε-martensite.

In addition, under rapid solidification conditions, it is expected that the development of excess vacancies will interact with lattice dislocations giving rise to osmotic forces on dislocations [**13**]. These forces are tremendously high and can result in dislocation climbing. Also, the condensation of excess vacancies along closed packed FCC planes can lead to prismatic vacancy loops which resemble intrinsic stacking faults. In turn, as mentioned before, these intrinsic stacking faults are likely to become potential fault defects for the spontaneous nucleation of athermal martensite [**14**].

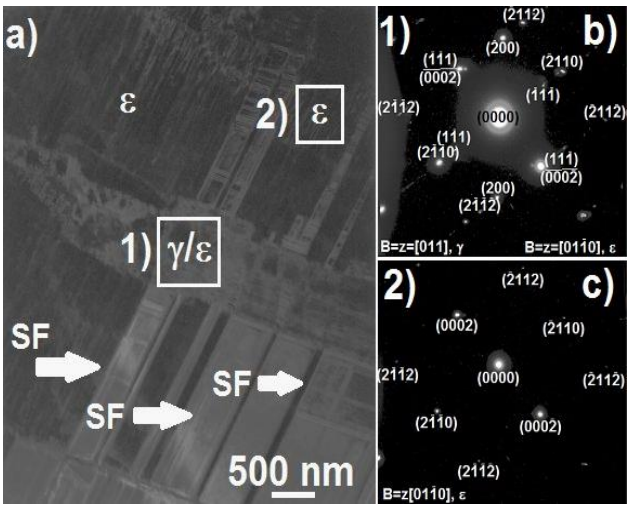

Fig. 4. Bright field micrograph of the as-cast Co-20Cr alloy showing a high percentage of ε-martensite.

Mechanical strength

Tensile testing indicated that the tensile strength in the rapidly solidified flat castings was of the order of 350 MPa, but it increased to values of up to 600 MPa after heat treating at 730ºC for 30 minutes (see **Fig. 5**). In addition the alloy ductility was relatively low but the heat treatment promoted a relatively high alloy ductility (i e from < 3 % to 27 %).

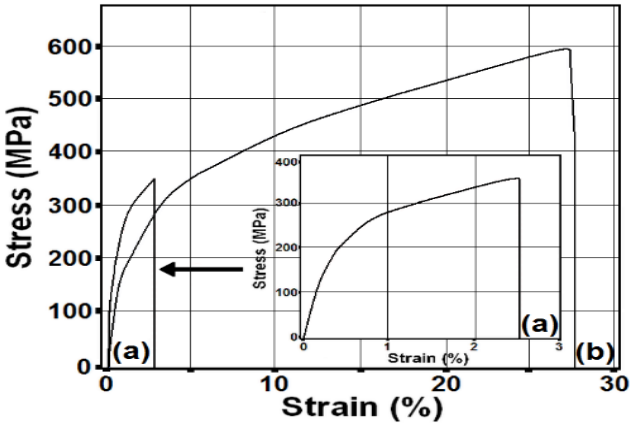

Fig. 5. Mechanical Strength and alloy ductility in the as-cast condition and after heat treating.

The alloy fracture path clearly shifts from low ductility interdendritic to the classic transgranular ductile path by microvoid coalescence (see **Figs. 6a-b**). Apparently, the rapidly solidified alloy was internally stressed as a result of extensive dislocation dissociation events and other non-equilibrium defects such as excess vacancies. In addition, upon ageing the alloy microstructure undergoes a change from athermal to isothermal ε−martensite with a concomitant improvement in the exhibited mechanical properties.

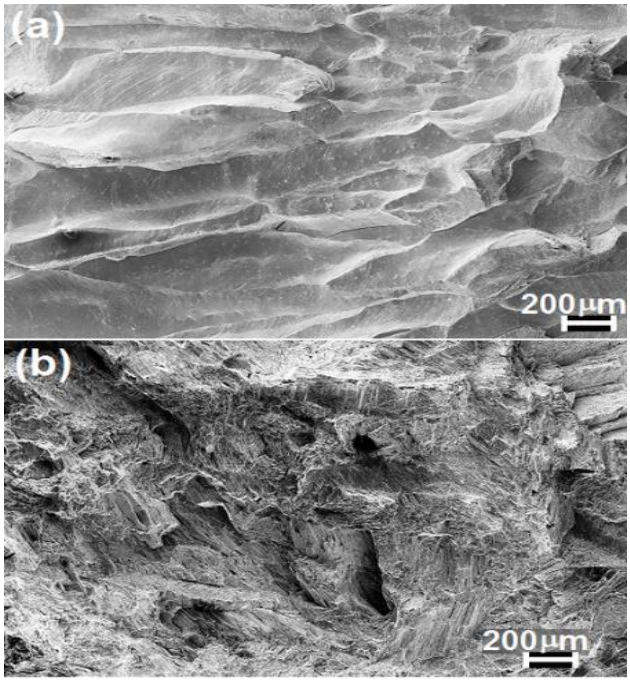

Fig. 6. Fracture surfaces of the Co-20Cr after tensile testing in (a) as-cast condition and (b) after heat treating.

Alloy biocompatibility

Fig. 7 shows potentiodynamic curves for the Co-20Cr alloy exposed to artificial saliva. From these preliminary results the exhibited corrosion current is of the order of $1x10^{-4}$ mA/cm2. Accordingly, it is apparent that the alloy biocompatibility in saliva is rather good and that the alloy can be used for potential tooth applications.

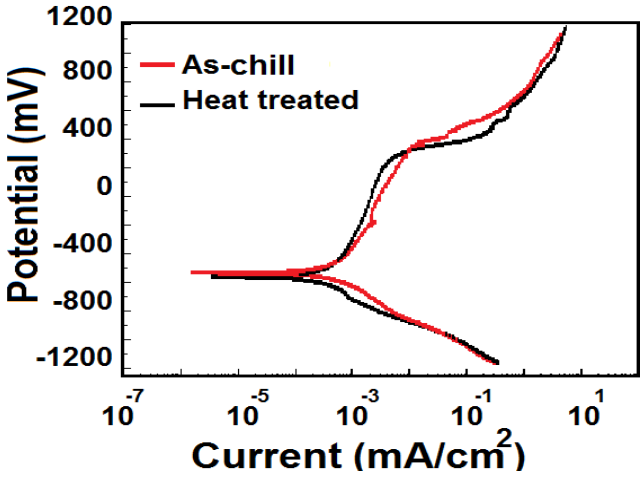

Fig. 7. Polarization curves for the Co-20 wt. % Cr alloy.

Yet, the corrosion properties are slightly reduced after heat treating. **Table 2** shows the exhibited corrosion properties of the alloy in both as-cast and after a heat treatment. Notice a slight increment in the corrosion current in the heat treated alloy.

Table 2: Corrosion properties from polarization curves.

Co-20wt. %Cr (condition)	E_{corr} (mV)	I_{corr} (mA/cm^2)	E_{pit} (mV)	I_{pit} (mA/m^2)	V_{corr} (mm/yr)
As-cast	-554.2	1 x 10^{-4}	298.2	0.006	0.00084
Heat treated	-524.19	4.22 x 10^{-4}	384.16	0.014	0.00356

This change in corrosion resistance is attributed to possible alloy segregation effects which are not present in the as-cast alloy during rapid solidification conditions. Ageing at 730ºC is likely to induce a redistribution of Cr in the alloy and consequently resulting in a reduction in corrosion resistance in artificial saliva.

Conclusion

1. Rapid solidification was induced in a an as-cast Co–20Cr by using water cooled V-shaped Cu-molds.
2. The fast heat dissipation during the thermal heat evolution lead to the development of significant amounts of athermal e-martensite (up to 90 %).
3. The alloy dendritic microstructure and exhibited segregation were greatly refined.
4. The corrosion properties were negatively influenced by the implemented heat treatment.

5. The mechanical strength and ductility significantly improved with the implemented HT

References

1. Lee, S.H.; Nomura, N.; Chiba, A.; *Mater. Trans. JIM*, **2008**, 49, 260.
2. Niinomi, M.; Nakai, M.; Hieda, J.; *Acta Biomater.* **2012**, 8, 3888.
3. Hedberg, Y.S.; Qian, B.; Shen, Z.; Virtanen, S.; Odnevall-Wallinder, I.; *Dent. Mater.* **2014**, 30, 525.
4. Vandamme, N.S.; Topoleski, L.D.T.; *J. Mater. Sci. Mater. Med.* **2005**, 16, 647.
5. Podrez-Radziszewska, M.; Haimann, K.; Dudziński, W.; Morawska-Sołtysik, M.; *Arch. Foundry Eng.* **2010**, 10, 51.
6. Carpenter Technology Corporation, Medical Implant Alloys, 12-95/4M, Reading PA.
7. K. Yamanaka K.; Mori M.; Chiba A.; *Acta Biomater*. **2013**, 9, 6259.
8. Yamanaka K.; Mori M.; Kurosu S.; Matsumoto H.; Chiba A.; *Metall. Mater. Trans. A*, **2009**, 40A, 1980.
9. López H.F.; Saldivar-Garcia A.J.; *Metall. Mater. Trans. A*, **2008**, 39A, 8.
10. Huang, P.; Salinas-Rodriguez, A.; Lopez, H.F.; *Mater. Sci. Technol.* **1999**, 15, 1324.
11. Ramirez-Ledesma A.L.; López H.F.; Juarez-Islas J.A.; *Metals*, 2016, 6, 188.
12. Saldivar-Garcia A.J.; Mani-Medrano A.; Salinas-Rodriguez A.;, *Scripta Mater*. **1999**, 40, 717.
13. Huang P.; López H.F., *Mater. Lett*. **1999**, 39, 249.
14. Olson G.B.; Cohen M.; *Metall. Trans. A*, **1976**, 7A, 1897.
15. Zangeneh Sh.; Ketabchi M.; López H.F.; *Mater. Lett.* **2014**, 116, 188.
16. Vega-Valer V.; MS Thesis, Department of Materials Science and Engineering, University of Wisconsin-Milwaukee (**2014**).
17. Sage M.; Gillaud C.; *Rev Metall*. **1950**, 49, 139.

